

Dependence of Temporal Properties on Energy in Long-Lag, Wide-Pulse Gamma-Ray Bursts

Fu-Wen Zhang^{1,4}, Yi-Ping Qin^{2,3} and Bin-Bin Zhang^{1,4,5}

¹*National Astronomical Observatories/Yunnan Observatory, Chinese Academy of Sciences, P.O. Box 110, Kunming, Yunnan 650011, China*

fwzhang@hotmail.com; fwzhang@ynao.ac.cn

²*Center for Astrophysics, Guangzhou University, Guangzhou 510006, China*

³*Physics Department, Guangxi University, Nanning, Guangxi 530004, China*

⁴*The Graduate School of the Chinese Academy of Sciences, P.O. Box 3908, Beijing 100039, China*

⁵*Department of Physics and Astronomy, University of Nevada, Las Vegas, NV 89154, USA*

(Received ; accepted)

Abstract

We employed a sample compiled by Norris et al. (2005, ApJ, 625, 324) to study the dependence of the pulse temporal properties on energy in long-lag, wide-pulse gamma-ray bursts. Our analysis shows that the pulse peak time, rise time scale and decay time scale are power law functions of energy, which is a preliminary report on the relationships between the three quantities and energy. The power law indexes associated with the pulse width, rise time scale and decay time scale are correlated and the correlation between the indexes associated with the pulse width and the decay time scale is more obvious. In addition, we have found that the pulse peak lag is strongly correlated with the CCF lag, but the centroid lag is less correlated with the peak lag and CCF lag. Based on these results and some previous investigations, we tend to believe that all energy-dependent pulse temporal properties may come from the joint contribution of both the hydrodynamic processes of the outflows and the curvature effect, where the energy-dependent spectral lag may be mainly dominated by the dynamic process and the energy-dependent pulse width may be mainly determined by the curvature effect.

Key words: gamma rays: bursts - method: statistical

1. Introduction

Cosmic gamma-ray bursts (GRBs) exhibit a great diversity of the temporal and spectral structure, and their origin and mechanism are still unclear. In many bursts the temporal

activity is suggestive of a stochastic process. It was suggested that some simple bursts with well-separated structure might consist of fundamental units of emission such as pulses, with some of them being seen to comprise a fast rise and an exponential decay (FRED) (see, e.g. Fishman 1994). The temporal and spectral properties of these fundamental pulses might give us valuable clues about the origin of these events and will provide powerful constraints on the detailed physical process.

Recently, the temporal and spectral characteristics of GRB pulses have been intensively studied, and several significant correlations between them have been found. Norris et al. (1986) first noted that GRB pulses have a general observed trend of hard to soft spectral evolution. This has been confirmed by many other authors (see, e.g., Bhat et al. 1994; Norris et al. 1996; Band 1997). The hard-to-soft spectral evolution are associated with two distinct, observed features: pulse peaks shift to later times and pulses become wider at lower energies (e.g., Link, Epstein, & Priedhorsky 1993; Norris et al. 1996; Norris, Narani & Bonnell 2000; Norris et al. 2005, hereafter Paper I). By using the average autocorrelation function and the average pulse width, Fenimore et al. (1995) showed that the narrowing of pulse width with energy well follow a power law, with an index of ~ -0.4 . This is the first quantitative relationship between the temporal and spectral structure in GRBs. Norris et al. (1996) proposed a “pulse paradigm” and found that the average raw pulse shape dependence on energy is also approximately a power law, consistent with the autocorrelation analysis of Fenimore et al. (1995). This was further confirmed by later studies (Piro et al. 1998; Costa 1999; Nemiroff 2000; Feroci et al. 2001; Crew et al. 2003; Qin et al. 2004; Qin et al. 2005; Peng et al. 2006).

In the standard fireball scenario, it was suggested that the process of radiation in GRBs is most likely through synchrotron emission (see, e.g., Katz 1994; Sari, Narayan, & Piran 1996). The power-law dependence of pulse width on energy has led to the suggestion that this relationship could be related with synchrotron radiation (Fenimore et al. 1995; Cohen et al. 1997; Piran 1999). Kazanas, Titarchuk, & Hua (1998) proposed that the result could be accounted for by synchrotron cooling (see also Chiang 1998; Dermer 1998; Wang et al. 2000). It was suspected that the power-law relationship might result from a relative projected speed or a relative beaming angle (Nemiroff 2000). Recently, it has been also argued that the relativistic curvature effect could lead to the power-law relationship (Qin et al. 2004; Qin et al. 2005; Shen, Song & Li 2005; Peng et al. 2006). Dado, Dar & De Rújula (2007) suggested that such correlation is a straightforward prediction of the ‘cannonball’ model of GRBs (Dar & De Rújula 2004).

The phenomenon of GRB pulse peaks evolving from higher to lower energies is a prevalent property of most bursts. Many authors generally analyze a time delay between the light curves in different energy bands. Using the cross-correlation method, Cheng et al. (1995) first found that soft emission had a time delay relative to high-energy emission and quantified the delay. Subsequently, several investigations on the GRB lag have been carried out (Norris et al.

1996; Norris, Narani & Bonnell 2000; Wu & Fenimore 2000; Hakkila & Giblin 2004; Hakkila & Giblin 2006; Chen et al. 2005; Norris & Bonnell 2006; Yi et al. 2006; Zhang et al. 2006b; Zhang et al. 2006c). There have been several attempts to explain the origin of the time lag. It was suggested that the activity of the central engine and hydrodynamic time-scale of the internal shocks might produce the time lag (e.g. Daigne & Mochkovitch 1998; 2003; Wu & Fenimore 2000). Ioka & Nakamura (2001) proposed that the lag was caused by the viewing angle of the jet. Another possible origin of the lag was proposed to be the radiative cooling (e.g. Zhang et al. 2002; Bai & Lee 2003; Schaefer 2004). Kocevski & Liang (2003) assumed that the observed lag was the direct result of spectral evolution (see also Ryde 2005). Shen, Song & Li (2005) argued that the observed lags could be accounted for by the curvature effect of fireballs (see also Lu et al. 2006).

Kocevski, Ryde & Liang (2003) found that there is a linear relationship between the pulse rise time and the pulse width (see figure 10 in the paper). The same result was also found in GRB pulses observed by the INTEGRAL (see figure 5a in Ryde et al. 2003). Recently, the strong correlation between the pulse rise time and the pulse width in different energy channels was presented by authors of Paper I. They fitted the two quantities with a power-law function and found that the slope increasing from 0.7 to 1.0 as the energy channel increases and the correlation is the tightest in channel 3 (100 – 300 keV). Lu, Qin & Yi (2006) further studied the relationship between the two quantities and proposed that merely the curvature effect could reproduce the correlation.

Although a power-law anti-correlation between pulse width and energy, a strong correlation between pulse rise time and pulse width, and pulse peaks evolve in time from higher to lower energies in many GRBs have been studied by many authors, it is unclear how the pulse peak time, rise time scale and decay time scale depend on energy. Recently, Liang et al. (2006) have tentatively investigated the correlation between the peak time and the average photon energy for GRB 060218, which has the longest pulse duration and spectral lag observed to date among the observed GRBs, and found that $t_{peak} \propto E^{-0.25 \pm 0.05}$. It is known that most bright bursts have many narrow pulses that are difficult to model due to overlapping. However, the relatively simple, long spectral lag, wide-pulse bursts are easier to model and might have simpler physics. Since the pulses in long-lag bursts are very long, the sufficient pulse definition is available, which makes the study easier. Authors of Paper I have analyzed the temporal and spectral behavior of wide pulses in 24 long-lag bursts, using a pulse model with two shape parameters, width and asymmetry, and the Band spectral model with three shape parameters. They found that the five descriptors are essentially uncorrelated, but pulse width is strongly correlated with spectral lag. They also found that pulses in long-lag bursts are distinguished from those in bright bursts: pulses in long spectral lag bursts are fewer in number and ~ 100 times wider (tens of seconds), have systematically lower peaks in νF_ν , and have significantly softer spectra.

As discovered in Norris (2002), proportion of long-lag, wide pulses within long-duration bursts increases from negligible among bright BATSE bursts to $\sim 50\%$ at the trigger threshold. Long-lag bursts appear to be important since these bursts may form a separate subclass of GRBs (Liang et al. 2007), and have relatively simple physical mechanism. Based on the fact that redshifts of three such bursts are available [GRB 980425 (Galama et al. 1998), 031203 (Malesani et al. 2004) and 060218 (Mirabal et al. 2006)], it was argued that long-lag bursts are probably relatively nearby, and the local event rate of these GRBs should be much higher than that expected from the high luminosity GRBs (Liang et al. 2007; Cobb et al. 2006; Pian et al. 2006; Soderberg et al. 2006). It was suggested that their wide-pulse, long-lag, and under-luminous features are partly attributed to the off-axis viewing angle effect (Nakamura 1999; Salmonson 2000; Ioka & Nakamura 2001), and partly due to their lower Lorentz factors (Kulkarni et al. 1998; Woosley & MacFadyen 1999; Salmonson 2000; Dai, Zhang & Liang 2006; Wang et al. 2006). Recently, it was argued that they might have a different type of central engine (e.g. neutron stars rather than black holes) from bright GRBs (Mazzali et al. 2006; Soderberg et al. 2006; Toma et al. 2007).

In this paper, we employ the long-lag burst sample investigated in Paper I to analyze the dependence of their temporal properties on energy. We describe the sample and data in section 2. The results are presented in section 3, followed by conclusions in section 4.

2. Sample and Data Description

The GRB sample employed is that presented in Paper I, where the bursts are found to consist of few long-lag, wide, well-defined pulses. The data are provided by the BASTE instruments on board the CGRO spacecraft. In this sample, obvious migration of peaks of the pulses in different energies can be observed. The bursts of the sample are from 1429 BATSE events described in Norris (2002), with the criterion that $T_{90} > 2$ s, $F_{peak} > 0.75$ photons $\text{cm}^{-2} \text{s}^{-1}$ (50-300 keV), peak intensity $PI > 1000$ counts s^{-1} (> 25 keV) and average lag > 1 s. In addition, only the bursts with sufficiently non-overlapping pulses are considered. The sample consists of 24 bursts, most of which contain single pulses. (For more details of the sample selection, see Paper I.)

For the purpose of fitting a pulse, authors in Paper I developed a pulse model with a form containing two exponentials, one increasing and one decreasing with time. This pulse model is written as $I(t) = A\lambda/[exp(\tau_1/t)exp(t/\tau_2)]$, where $\lambda = exp[2(\tau_1/\tau_2)^{1/2}]$, A is the pulse peak intensity, and τ_1 and τ_2 are the two fundamental timescales dominating the rise and decay rates, respectively. The time of pulse onset with respect to $t = 0$, t_s , is ignored. The 24 long-lag bursts were fitted with this model in Paper I. Parameter values for all identified pulses were obtained, including pulse peak intensity (A), pulse onset time (t_s), effective onset time (t_{eff}), peak time (τ_{peak}), the two fundamental timescales (τ_1 and τ_2), width (w) and asymmetry (k) (see Table 2 in Paper I). The corresponding errors were also estimated. The effective onset

time, t_{eff} , is defined as the time when the pulse reaches 0.01 times of the peak intensity. Both onset times are relative to the burst trigger time. The peak time is defined as that relative to the effective onset time.

3. Results

Due to a variety of interpretation of the spectral lag observed in GRBs, we suspect that the quantity might be contributed by various effects. The most important one might be the mechanism of shocks which are likely to dominate light curves of pulses in their rise phase. Another important factor might be the curvature effect which seems to dominate the decay phase of pulses (see, e.g., Qin & Lu 2005). We thus pay our attention on how the pulse peak time, rise and decay time scales depending on energy, checking if the dependence is the same or different.

3.1. Dependence of pulse peak time, rise time and decay time scales on energy

To investigate this issue, let us define three quantities: pulse peak time position (t_p), pulse rise time scale (Δt_r) and pulse decay time scale (Δt_d), where t_p is defined as the time between the pulse peak and the pulse onset, Δt_r and Δt_d are defined as the time between the pulse peak and the two $1/e$ intensity points respectively as those defined in Paper I. (Note that Δt_r and Δt_d are close to the FWHMs in the rising phase and decaying phase respectively, since $1/e$ is close to $1/2$. In addition, according to their definitions, $\Delta t_r = \tau_{rise}$ and $\Delta t_d = \tau_{dec}$, where τ_{rise} and τ_{dec} are the pulse rise and decay timescales defined in Paper I, respectively.) The onset time, t'_s , defined here is the time (relative to the burst trigger time) when the total counting rate of all four energy channels (25 – 50, 50 – 100, 100 – 300, and > 300 keV) reaches 0.01 times the peak intensity in a single-pulse burst. With this definition, the pulse peak time positions, t_p , in the different channels for a burst are relative to the same reference time (the onset t'_s). We thus can directly compare them (or, the shifts of the pulse peaks with respect to the different channels can be easily estimated). The τ_{peak} listed in Table 2 of Paper I is relative to t_{eff} (for a same burst, values of t_{eff} are different in the different energy channels), which is nothing but a measure of the pulse rise time as described in Paper I. The peak time position t_p is merely a shift of τ_{peak} of individual pulse, but for a burst the shifting steps are different in the different channels.

We employ all GRBs presented in Paper I to study the dependence of t_p , Δt_r and Δt_d on energy. For each burst we require that the pulse signal should be detectable in at least three channels (in this way, the relationship between these quantities and energy can be studied). Pulses of the same burst being blended, such as the three pulses in the burst of #2711, are not included. With these requirements, we obtain 24 pulses which belong to 23 bursts. In the analysis of the relationship between t_p and energy, we only consider the single-pulse bursts since the onset is well determined. The burst of #8049 is excluded.

Parameters of the model described by equation (1) in Paper I for the 24 pulses in different energy channels are available in Table 2 of the paper. According to equation (2) of Paper I, $\Delta t_r + \Delta t_d$ ($\Delta t_r + \Delta t_d = w$) could be determined by τ_1 and τ_2 . We thus obtain Δt_r and Δt_d for the 24 pulses in different energy channels from that table via a simple derivation. Listed in Table 2 of Paper I is also the effective onset time t_{eff} defined in that paper, which is relative to the trigger time, for each pulse in each channel. With t_{eff} and τ_{peak} we are able to determine the pulse peak time relative to the trigger time. We combine the 64 ms count data from all four channels (the data are available via anonymous ftp in the website¹) to obtain the “bolometric” light-curve profile, and derive our onset time t'_s for each burst by fitting the light curve with the method of Paper I, where the adopted pulse model is equation (1) of the paper. Shifting τ_{peak} from t_{eff} to t'_s yields the peak time t_p defined in this paper. The correspondent uncertainties are calculated through the error transfer formula.

Illustrated in Figure 1 are t_p , Δt_r and Δt_d of individual pulses in each energy channel. To compare with the dependence of the pulse width on energy, the value of Δt_w , which is defined as the time between the two $1/e$ intensity points of individual pulse as that defined in Paper I ($\Delta t_w = w$), of each pulse is also displayed in Figure 1. The figure shows clearly that t_p generally migrates to later times at lower energy channels, and Δt_w , Δt_r and Δt_d become wider at lower energy bands (in several exception cases, the data points are well inside the corresponding trend within 1σ errors).

According to Figure 1, we assume that the four time quantities t_p , Δt_w , Δt_r , and Δt_d are power law functions of energy. The dependence of the four time quantities on energy is parameterized by the power law index which is obtained by fitting the data points of each quantity in the four energy channels with a power law. The energy adopted for a channel is the geometric mean of the lower and upper boundaries of the channel (here we use 300 – 1000 keV for channel 4, which is adopted throughout this paper). This method of analysis was generally adopted in previous works (see, Fenimore et al. 1995; Norris et al. 1996; Paper I). Let α_p , α_w , α_r , and α_d denote the indices of the power law relationships between t_p , Δt_w , Δt_r , and Δt_d and energy, respectively. Displayed in Figure 2 are the distributions of these indices. We fit them with a Gaussian. Values of the fit (the standard deviation) as well as the medians of the distributions of the four power-law indices are listed in Table 1. [For the distribution and other analysis of α_w , see also Jia & Qin (2005); Peng et al. (2006).] One can find from Figure 2 and Table 1 that the distributions of these indices have large dispersions. This implies that the energy dependence of the temporal properties may not be the same for different bursts. It is interesting that the distribution of α_r is obviously narrower than that of other indices (see Table 1). A possible interpretation to this phenomenon is that the mechanism causing the dependence of the rise time scale on energy might be somewhat similar for different bursts.

In the analysis of the relationship between the pulse width and energy, one generally

¹ <ftp://coss.c.gsfc.nasa.gov/compton/data/batse/>

studied the dependence of the average pulse width on energy for the adopted samples (see, for example, Fenimore et al. 1995; Norris et al. 1996; Paper I). Here, we also calculate the dependence of the average values of t_p , Δt_r and Δt_d on energy. For the sake of comparison, the energy dependence of the average value of Δt_w is displayed as well (we include only those bursts with their pulse signal being detectable in all four channels; the burst of #6526, which has a very long timescale, is excluded throughout the paper). Plotted in Figure 3 are the relationships between the average values of t_p , Δt_w , Δt_r , Δt_d and energy. The regression analysis yields: $\log t_p = (1.45 \pm 0.26) - (0.25 \pm 0.14)\log E$, $\log \Delta t_w = (2.15 \pm 0.09) - (0.45 \pm 0.05)\log E$, $\log \Delta t_r = (1.40 \pm 0.10) - (0.37 \pm 0.05)\log E$ and $\log \Delta t_d = (2.08 \pm 0.09) - (0.48 \pm 0.05)\log E$.

3.2. Relationships between power-law indices

As power law indices are an active factor reflecting the relationship between the temporal and spectral properties of pulses, we are curious about how the three power-law indices, α_w , α_r and α_d , which are associated with various widths of pulses, are related. Figure 4 shows the relations between them. Results of the correlation analysis for the three quantities are listed in Table 2. We find that α_w and α_d are highly correlated, while the other pairs of the quantities are obvious less correlated. It suggests that the mechanism causing the power law relationship between the pulse width and energy is the same as that between the pulse decay time scale and energy. Recall that, the distributions of these indices have large dispersions which implies that the energy dependence of these temporal properties may not be the same for different bursts. We guess that the energy dependence of the rise time scale and that of the decay time scale for the same burst during the same pulse might share some mechanism which is unclear currently. If this mechanism varies from burst to bursts, there would exist a weak correlation between α_r and α_d as observed in Figure 4.

Shown in other aspects, correlation analysis between Δt_r , Δt_d and Δt_w in different energy channels might be helpful. The results are illustrated in Figure 5 which shows that Δt_r , Δt_d and Δt_w are correlated and the strong correlations between Δt_d and Δt_w exist in each of the three energy channels. This is consistent with the previous studies (Kocevski, Ryde & Liang 2003; Ryde et al. 2003; Lu, Qin & Yi 2006). What hinted and concluded by the correlation analysis of the indices are reinforced by these new results. One should keep in mind that correlations between different temporal properties might partially (or mainly) be due to the same Lorentz factor for the same pulse (see, Lu, Qin & Yi 2006), but the more obvious correlation between Δt_d and Δt_w than that between other pairs suggests that, besides the Lorentz factor, there must be other factors at work in producing the strong correlation between the two quantities. As shown in Zhang & Qin (2005), the ratio of $FWHM_r$ to $FWHM_d$ is not affected by the Lorentz factor.

One might notice that, in terms of mathematics, the strong correlations between α_d and α_w and between Δt_d and Δt_w may result from the fact that Δt_w is dominated by Δt_d . Or, in

turn, the strong correlations between α_d and α_w and between Δt_d and Δt_w may confirm the fact. As shown in Qin et al. (2004), the ratio of $FWHM_r$ to $FWHM_d$ would be less than 1.3 for pulses arising from the emission of relativistically expanding fireballs. Therefore, it is expected that Δt_w might generally be dominated by Δt_d , as what suggested in Figure 1.

From Figures 2 and 4 one finds that $\alpha_d < \alpha_r$. This suggests that the decay time scale rapidly decreases with respect to energy, while the variance of the rise time scale with the increasing of energy is relatively mild. Is it implying that the curvature effect plays an important role in the decaying phase of pulses and the contribution of the effect makes α_d smaller (see, e.g., Qin et al. 2005; Peng et al. 2006)?

3.3. Relationships between various spectral lags and between the lags and other time scales

Authors of Paper I measured the peak lags of all pulses between channels 2 and 3 in 24 long-lag bursts, and found that as pulse width increases, the spectral lag measured between pulse peaks tends to increase. We find that not only the peak time lag (note that what we measure here is the peak lag between channels 1 and 3, $\tau_{p,13}$) but also the CCF lag, which is the lag calculated with the cross correlation function (CCF) method, increase with the increasing of the pulse width (the figure is omitted). The CCF lag used here is also derived between channels 1 and 3, $\tau_{CCF,13}$, which has been extensively studied (Link, Epstein, & Priedhorsky 1993; Cheng et al. 1995; Norris et al. 1996; Norris, Narani & Bonnell 2000; Wu & Fenimore 2000; Hakkila & Giblin 2004; Hakkila & Giblin 2006; Chen et al. 2005; Norris & Bonnell 2006; Yi et al. 2006; Zhang et al. 2006b; Zhang et al. 2006c). Here, we derive the CCF lag from the peak of the CCF without considering the side lobe contribution of the CCF. Since the light curves are the smooth pulses and their lags are significantly larger than the time bin, the peaks of CCFs are robust to estimate the lags. The errors of CCF lags are evaluated by simulations. Besides these two lags, the centroid lag which is the lag of the pulse centroid was discussed in Paper I, and it was found to be well measured and to be well correlated with the pulse width. It was suggested recently that the correlation might be due to the Lorentz factor (see, e.g. Peng et al. 2007).

To analyze the relationships between the three lags, we calculate the centroid lag between channels 1 and 3 ($\tau_{cen,13}$) as well. The plots of $\tau_{cen,13}$ vs. $\tau_{p,13}$, $\tau_{cen,13}$ vs. $\tau_{CCF,13}$, and $\tau_{CCF,13}$ vs. $\tau_{p,13}$ are displayed in Figure 6. One finds that $\tau_{cen,13}$ is weakly correlated with both $\tau_{p,13}$ and $\tau_{CCF,13}$, while the later two are strongly correlated. The best fits to $\tau_{CCF,13}$ and $\tau_{p,13}$ yields $\log\tau_{CCF,13} = (-0.25 \pm 0.06) + (1.18 \pm 0.11)\log\tau_{p,13}$. The strong correlation between $\tau_{p,13}$ and $\tau_{CCF,13}$ and the weak correlations between the two quantities and $\tau_{cen,13}$ suggest that $\tau_{CCF,13}$ is mainly caused by the shifting of peaks while $\tau_{cen,13}$ is not. We believe that $\tau_{p,13}$ and $\tau_{cen,13}$ reflect different aspects of spectral lags, with one representing the shifting of peaks and the other describing the enhancement of the time scale of pulses. We thus propose that, to reveal a spectral lag in detail, both $\tau_{p,13}$ and $\tau_{cen,13}$ should be measured.

In addition, we find that $\tau_{cen,13}$ is systematically larger than both $\tau_{p,13}$ and $\tau_{CCF,13}$. According to the above interpretation, this implies that the lag caused by the stretching of pulses is always larger than that caused by the shifting of peaks.

Hakkila & Giblin (2006) found that GRB lags are consistent across a wide range of prompt emission energies, $lag_{31} \approx lag_{21} + lag_{32}$. Under the interpretation proposed above, the three lags, lag_{31} , lag_{21} and lag_{32} are mainly due to the shifting of t_p in the corresponding channels. Therefore, they could be approximated by $\tau_{p,13}$, $\tau_{p,12}$ and $\tau_{p,23}$, respectively. Meanwhile, according to their definitions, one has $\tau_{p,13} = \tau_{p,12} + \tau_{p,23}$. The relation $lag_{31} \approx lag_{21} + lag_{32}$ is thus explained.

Bhat et al. (1994) found that the time lag between the counting rate and the hardness ratio was directly correlated with the rise time of the burst counting rate profile. Motivated by this, we analyze the relationships between the three lags and the pulse rise time and decay time scales. The results are displayed in Figure 7. It shows that the peak lag and CCF lag are well correlated with the pulse rise time scale and weakly correlated with the pulse decay time scale, which is consistent with that found by Peng et al. (2007). However, the centroid lag is strongly correlated with the pulse decay time scale and weakly correlated with the pulse rise time scale. The latter phenomenon is in agreement with what interpreted above. As discussed in last subsection, Δt_w is likely dominated by Δt_d . Thus, it is expectable that $\tau_{cen,13}$ is correlated with Δt_d , since according to the interpretation, the centroid lag reflects the stretching of the pulse width. The correlations between the peak and CCF lags and the pulse rise time scale indicate that the two lags might be caused by some mechanism associated with the pulse rise time scale. Probably, the peak and CCF lags and the pulse rise time scale might be created mainly by a dynamic process, while the centroid lag and the pulse decay time scale might be formed by both the dynamic process and the curvature effect.

4. Conclusions

Using the sample of 24 long-lag, wide-pulse GRBs described in Paper I, we have investigated the dependence of the pulse temporal properties on energy. It is obvious that the peak time generally migrates to later time at lower energy channels, and the pulse width, rise time and decay time scales become wider at lower energy bands. Fitting the average pulse peak time, rise time and decay time scales with a power law function of energy yields $t_p \propto E^{-0.25 \pm 0.14}$, $t_r \propto E^{-0.37 \pm 0.05}$ and $t_d \propto E^{-0.48 \pm 0.05}$. This is a preliminary report on the relationships between the three quantities and energy. The three power law indices α_p , α_r and α_d have large dispersions, and the medians of their distributions are -0.27 , -0.35 and -0.37 , respectively. It is not surprising since in the well defined power law relationship between the pulse width and energy one also finds a large dispersion of the index (see also Jia & Qin 2005; Peng et al. 2006). This implies that the energy dependence of the temporal properties may not be the same for different bursts. It is interesting that the distribution of α_r is obviously narrower

than that of other indices (see Table 1). A possible interpretation to this phenomenon is that the mechanism causing the dependence of the rise time scale on energy might be somewhat similar for different bursts. Liang et al. (2006) noted that the peak time dependence on the average energy (from 0.3-150 keV) in the single pulse burst GRB 060218 detected by Swift was approximately a power law, and the power law index was $\sim -0.25 \pm 0.05$, which is consistent with our result. This favors what argued by Liang et al. (2006) that this event may be a typical long-lag, wide-pulse burst and share the similar radiation physics with other BATSE bursts.

We also find that the three power-law indices α_w , α_r and α_d are correlated, where α_w and α_d are found to be more obviously correlated. It suggests that the mechanism causing the power law relationship between the pulse width and energy is the same as that between the pulse decay time scale and energy. Recalling that the distributions of these indices have large dispersions, implying that the energy dependence of these temporal properties may not be the same for different bursts, we guess that the energy dependence of the rise time scale and that of the decay time scale for the same burst during the same pulse might share some mechanism which is unclear currently. If this mechanism varies from burst to bursts, there would exist a weak correlation between α_r and α_d as observed in Figure 4.

In addition, we find that the pulse peak lag is strongly correlated with the CCF lag, but the centroid lag is weakly correlated with the peak lag and CCF lag. This suggests that the CCF lag is mainly caused by the shifting of peaks while the centroid lag is not. We argue that the peak lag and the centroid lag reflect different aspects of spectral lags, with one representing the shifting of peaks and the other describing the enhancement of the time scale of pulses. We thus propose that, to reveal a spectral lag in detail, both the peak lag and the centroid lag should be measured. Our analysis also shows that the centroid lag is systematically larger than both the peak and CCF lags. According to the above interpretation, this implies that the lag caused by the stretching of pulses is always larger than that caused by the shifting of peaks. According to the definition of the pulse peak lag and the relation between the peak time and energy, one has $\tau_{p,13} = \tau_{p,12} + \tau_{p,23}$. Along with the relationship between the peak lag and CCF lag, the relation $lag_{31} \approx lag_{21} + lag_{32}$ found by Hakkila & Giblin (2006) can be explained.

According to Ryde & Petrosian (2002), the simplest scenario accounting for the observed GRB pulses is to assume an impulsive heating of the leptons and a subsequent cooling and emission. In this scenario, the rising phase of the pulse, which is referred to as the dynamic time (the crossing time), arises from the energizing of the shell, while the decay phase is due to geometric and relativistic effects in an outflow with a Lorentz factor of $\Gamma \gtrsim 100$. An intuitive speculation is that the dependence of the pulse rise time on energy is attributed to hydrodynamic processes. In the internal shock model of GRB pulses, there are three contributors to the pulse temporal structure: cooling, hydrodynamics, and angular spreading timescales (Piran 1999; Piran 2005; Mészáros 2002; Mészáros 2006; Zhang & Mészáros 2004). Thus, the resulting time profile is a convolution of the three processes. Based on the current model which requires

a much stronger magnetic field and thus leads to very fast cooling, the typical cooling timescale ($\sim 10^{-6}$ s, see Wu & Fenimore 2000) is much shorter than the observed pulse delays, and hence the cooling timescale can not dominates the pulse profile. The effect of the angular time arising from kinematics, the so-called curvature effect, on the characteristics of pulses has been intensively studied (Panaitescu & Kumar 2002; Qin 2002; Ryde & Petrosian 2002; Kocevski, Ryde & Liang 2003; Dermer 2004; Dyks, Zhang & Fan 2005; Zhang et al. 2006a). It was argued that the curvature effect might be responsible for the spectral lag (Salmonson 2000; Ioka & Nakamura 2001; Shen, Song & Li 2005; Ryde 2005; Lu et al. 2006). The relationship between the pulse width and energy could also be accounted for by the curvature effect (Qin et al. 2004; Qin et al. 2005; Peng et al. 2006). However, Shen, Song & Li (2005) found that the curvature causes an energy-dependent pulse width distribution but the energy dependence of the width they obtained was much weaker than the observed $W \propto E^{-0.4}$ one. Yi et al. (2006) also argued that the curvature effect alone could not explain the difference of the spectral lags (see also Shen, Song, & Li 2005; Lu et al. 2006). Daigne & Mochkovitch(1998, 2003) developed a model in the framework of internal shock model (Rees & Mészáros 1994) and found that if GRB pulses were produced by internal shocks, their temporal and spectral properties were probably governed by the hydrodynamics of the flow rather by the geometry of the emitting shells. Recently, Lu et al. (2007) tentatively analyzed the origination of GRB pulses and found that the decay phase of the observed pulse originates from the contributions of both the curvature effect and the width of the intrinsic pulse, and the rising phase of the observed pulses only comes from the width of the intrinsic pulse (here the width of the intrinsic pulse is referred to as the dynamic time). We argue that all energy-dependent pulse temporal properties discussed above might probably come from the joint contribution of both the hydrodynamic processes of the outflows and the curvature effect, where the energy-dependent spectral lag may be mainly dominated by the dynamic process and the energy-dependent pulse width may be mainly determined by the curvature effect.

We appreciate the anonymous referee for her/his helpful suggestions. We thank Jinming Bai and Enwei Liang for their helpful discussions. This work is supported by National Natural Science Foundation of China (No. 10573030 and No. 10463001).

References

- Bai, J. M., & Lee, M. G. 2003, *ApJ*, 585, L113
 Band, D. L. 1997, *ApJ*, 486, 928
 Bhat, P. N., et al. 1994, *ApJ*, 426, 604
 Chen, L., Lou, Y. Q., Wu, M., Qu, J.-L., Jia, S.-M., & Yang, X.-J. 2005, *ApJ*, 619, 983
 Cheng, L. X., Ma, Y. Q., Cheng, K. S., Lu, T., & Zhou Y. Y. 1995, *A&A*, 300, 746
 Chiang, J., 1998, *ApJ*, 508, 752
 Cobb, B. E., Bailyn, C. D., van Dokkum, P. G., & Natarajan, P. 2006, *ApJ*, 645, L113

- Cohen, E., Katz, J. I., Piran, T., & Sari, R. 1997, *ApJ*, 488, 330
- Costa, E. 1999, *Nucl. Pphys. B (Proc. Suppl.)*, 69, 646
- Crew, G. B., et al. 2003, *ApJ*, 599, 387
- Dado, S., Dar, A., & De Rújula, A. 2007, *ApJ*, 663, 400
- Dar, A., & De Rújula, A. 2004, *Physics Reports*, 405, 203
- Dai, Z. G, Zhang, B., & Liang, E. W. 2006, preprint (astro-ph/0604510)
- Daigne, F., & Mochkovitch, R. 1998, *MNRAS*, 296, 275
- Daigne, F., & Mochkovitch, R. 2003, *MNRAS*, 342, 587
- Dermer, C. D. 1998, *ApJ*, 501, L157
- Dermer, C. D., 2004, *ApJ*, 614, 284
- Dyks, J., Zhang, B., & Fan, Y. Z. 2005, submitted (astro-ph/0511699)
- Fenimore, E. E., in 't Zand, J. J. M., Norris, J. P., Bonnell, J. T., & Nemiroff, R. J. 1995, *ApJ*, 448, L101
- Feroci, M., et al. 2001, *A&A*, 378, 441
- Fishman, G. J., et al. 1994, *ApJS*, 92, 229
- Galama, T. J., et al. 1998, *Nature*, 395, 670
- Hakkila, J., & Giblin, T. W. 2004, *ApJ*, 610, 361
- Hakkila, J., & Giblin, T. W. 2006, *ApJ*, 646, 1086
- Ioka, K., & Nakamura, T. 2001, *ApJ*, 554, L163
- Jia, L.-W., & Qin, Y.-P. 2005, *ApJ*, 631, L25
- Katz, J. I. 1994, *ApJ*, 422, 248
- Kazanas, D., Titarchuk, L. G., & Hua, X. M. 1998, *ApJ*, 493, 708
- Kocevski, D., & Liang, E. 2003, *ApJ*, 594, 385
- Kocevski, D., Ryde, F., & Liang, E. 2003, *ApJ*, 596, 389
- Kulkarni, S. R., et al. 1998, *Nature*, 395, 663
- Liang E. W., Zhang, B. B., Stamatikos, M., Zhang, B., Norris, J., Gehrels, N., Zhang, J., & Dai, Z. G. 2006, *ApJ*, 653, L81
- Liang, E. W., Zhang, B., Virgili, F., & Dai, Z. G. 2007, *ApJ*, 662, 1111
- Link, B., Epstein, R. I., & Priedhorsky, W. C. 1993, *ApJ*, 408, L81
- Lu, R.-J., Qin, Y.-P., & Yi, T.-F. 2006, *ChJAA*, 6, 52
- Lu, R.-J., Qin, Y.-P., & Zhang, F.-W. 2007, *ChPhy*, 16, 1806
- Lu, R.-J., Qin, Y.-P., Zhang, Z.-B., & Yi, T.-F. 2006, *MNRAS*, 367, 275
- Malesani, D., et al. 2004, *ApJ*, 609, L5
- Mazzali, P. A. et al. 2006, *Nature*, 442, 1018
- Mészáros, P. 2002, *ARA&A*, 40, 137
- Mészáros, P. 2006, *Rep. Prog. Phys.*, 69, 2259
- Mirabal, N., Halpern, J. P., An, D., Thorstensen, J. R., & Terndrup, D. M. 2006, *ApJ*, 643, L99
- Nakamura, T. 1999, *ApJ*, 522, L101
- Nemiroff, R. J. 2000, *ApJ*, 544, 805
- Norris, J. P., Share, G. H., Messina, D. C., Dennis, B. R., Desai, U. D., Cline, T. L., Matz, S. M., & Chupp, E. L. 1986, *ApJ*, 301, 213

- Norris, J. P., Nemiroff, R. J., Bonnell, J. T., Scargle, J. D., Kouveliotou, C., Paciesas, W. S., Meegan, C. A., & Fishman, G. J. 1996, *ApJ*, 459, 393
- Norris, J. P., Marani, G. F., & Bonnell, J. T. 2000, *ApJ*, 534, 248
- Norris, J. P. 2002, *ApJ*, 579, 386
- Norris, J. P., Bonnell, J. T., Kazanas, D., Scargle, J. D., Hakkila, J., & GIBLIN, T. W. 2005, *ApJ*, 627, 324 (Paper I)
- Norris, J. P., & Bonnell, J. T. 2006, *ApJ*, 643, 266
- Panaiteescu, A., & Kumar, P. 2002, *ApJ*, 571, 779
- Peng, Z.-Y., Qin, Y.-P., Zhang, B.-B., Lu, R.-J., Jia, L.-W., & Zhang, Z.-B. 2006, *MNRAS*, 368, 1351
- Peng, Z.-Y., Lu, R.-J., Qin, Y.-P., & Zhang B.-B. 2007, *ChJAA*, 7, 428
- Pian, E., et al. 2006, *Nature*, 442, 1011
- Piran, T. 1999, *Phys. Rep.*, 314, 575
- Piran, T. 2005, *Rev. Mod. Phys.*, 76, 1143
- Piro, L., et al. 1998, *A&A*, 329, 906
- Qin, Y.-P. 2002, *A&A*, 396, 705
- Qin, Y.-P., Zhang, Z.-B., Zhang, F.-W., & Cui, X.-H. 2004, *ApJ*, 617, 439
- Qin, Y.-P., Dong, Y.-M., Lu, R.-J., Zhang, B.-B., & Jia, L.-W. 2005, *ApJ*, 632, 1008
- Qin, Y.-P., & Lu, R.-J. 2005, *MNRAS*, 362, 1085
- Rees, M. J., & Mészáros, P. 1994, *ApJ*, 430, L93
- Ryde, F., & Petrosian, V. 2002, *ApJ*, 578, 290
- Ryde F., Borgonovo, L., Larsson, S., Lund, N., von Kienlin, A., & Lichti, G. 2003, *A&A*, 411, L331
- Ryde, F. 2005, *A&A*, 429, 869
- Salmonson, J. D. 2000, *ApJ*, 544, L115
- Sari, R., Narayan, R., & Piran, T. 1996, *ApJ*, 473, 204
- Schaefer, B. 2004, *ApJ*, 602, 306
- Shen, R. F., Song, L. M., & Li, Z. 2005, *MNRAS*, 362, 59
- Soderberg, A. M., et al. 2006, *Nature*, 442, 1014
- Toma, K., Ioka, K., Sakamoto, T., & Nakamura, T. 2007, *ApJ*, 659, 1420
- Wang, J. C., Cen, X. F., Qian, T. L., Xu, J., & Wang, C. Y. 2000, *ApJ*, 532, 267
- Wang, X.-Y., Li, Z., Waxman, E., & Meszaros, P. 2006, *ApJ*, in press (astro-ph/0608033)
- Wosley, S. E., & MacFadyen, A. I. 1999, *A&AS*, 138, 499
- Wu, B., & Fenimore E. 2000, *ApJ*, 535, L29
- Yi, T. F., Liang, E. W., Qin, Y. P., & Lu, R. J. 2006, *MNRAS*, 367, 1751
- Zhang, B., & Mészáros, P. 2004, *Int. J. Mod. Phys. A*, 19, 2385
- Zhang, B., Fan, Y. Z.; Dyks, J., Kobayashi, S., Mészáros, P., Burrows, D. N., Nousek, J. A., & Gehrels, N. 2006a, *ApJ*, 642, 354
- Zhang, F.-W., & Qin, Y.-P. 2005, *Chin. Phys.*, 14, 2276
- Zhang, Y. H., et al. 2002, *ApJ*, 572, 762
- Zhang, Z., Xie, G. Z., Deng, J. G., & Jin, W. 2006b, *MNRAS*, 373, 729
- Zhang, Z.-B., Deng, J.-G., Lu, R.-J., & Gao, H.-F. 2006c, *ChJAA*, 6, 312

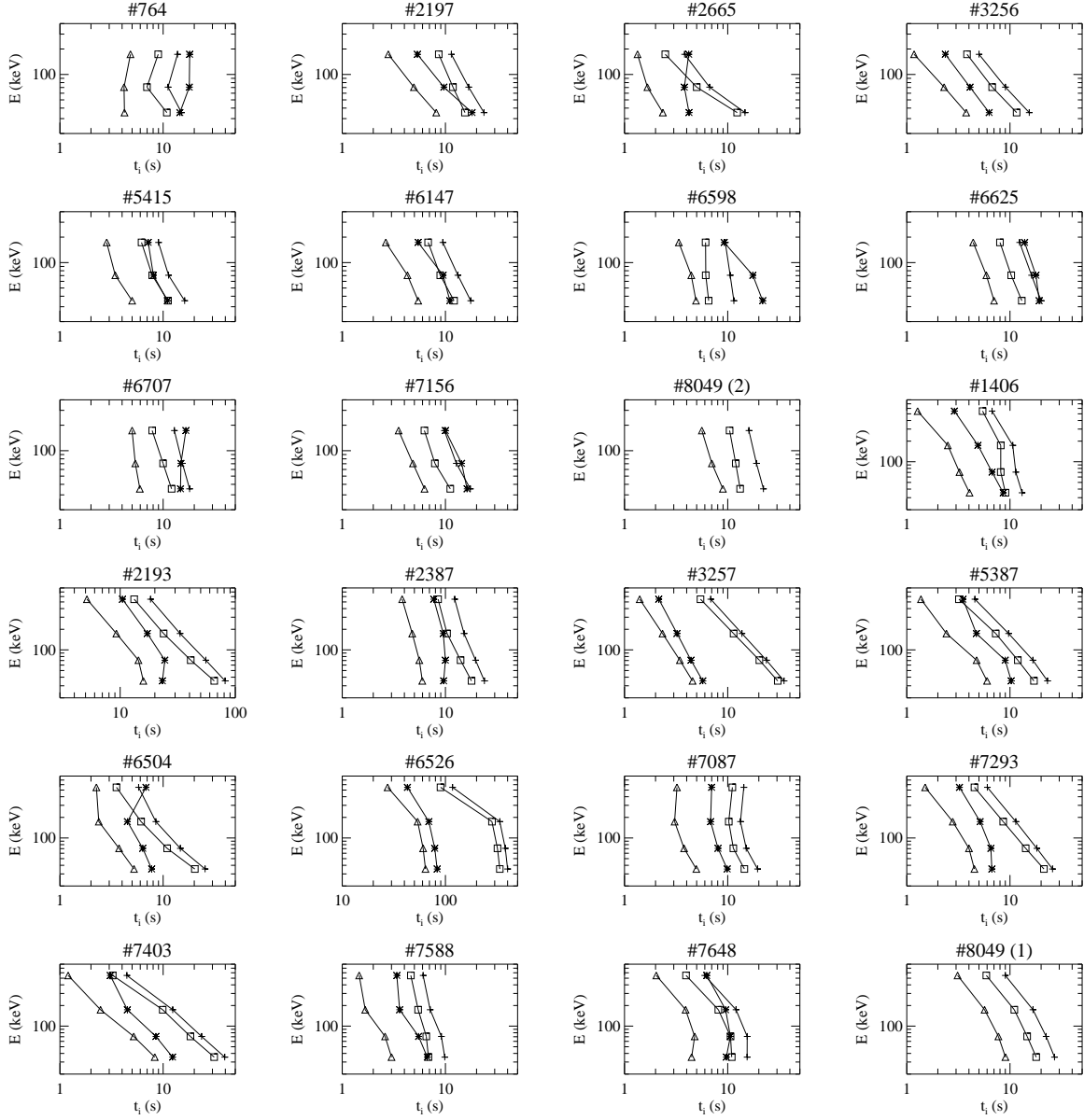


Fig. 1. Energy vs. pulse peak time (asterisk), pulse width (cross), pulse rise time scale (open triangle) and pulse decay time scale (open square) for all the 24 pulses studied in this paper, where E is the geometric means of the lower and upper channel boundaries, t_i represents t_p , Δt_w , Δt_r and Δt_d . Symbols joined by line segments correspond to the same time quantity in the different energy channels.

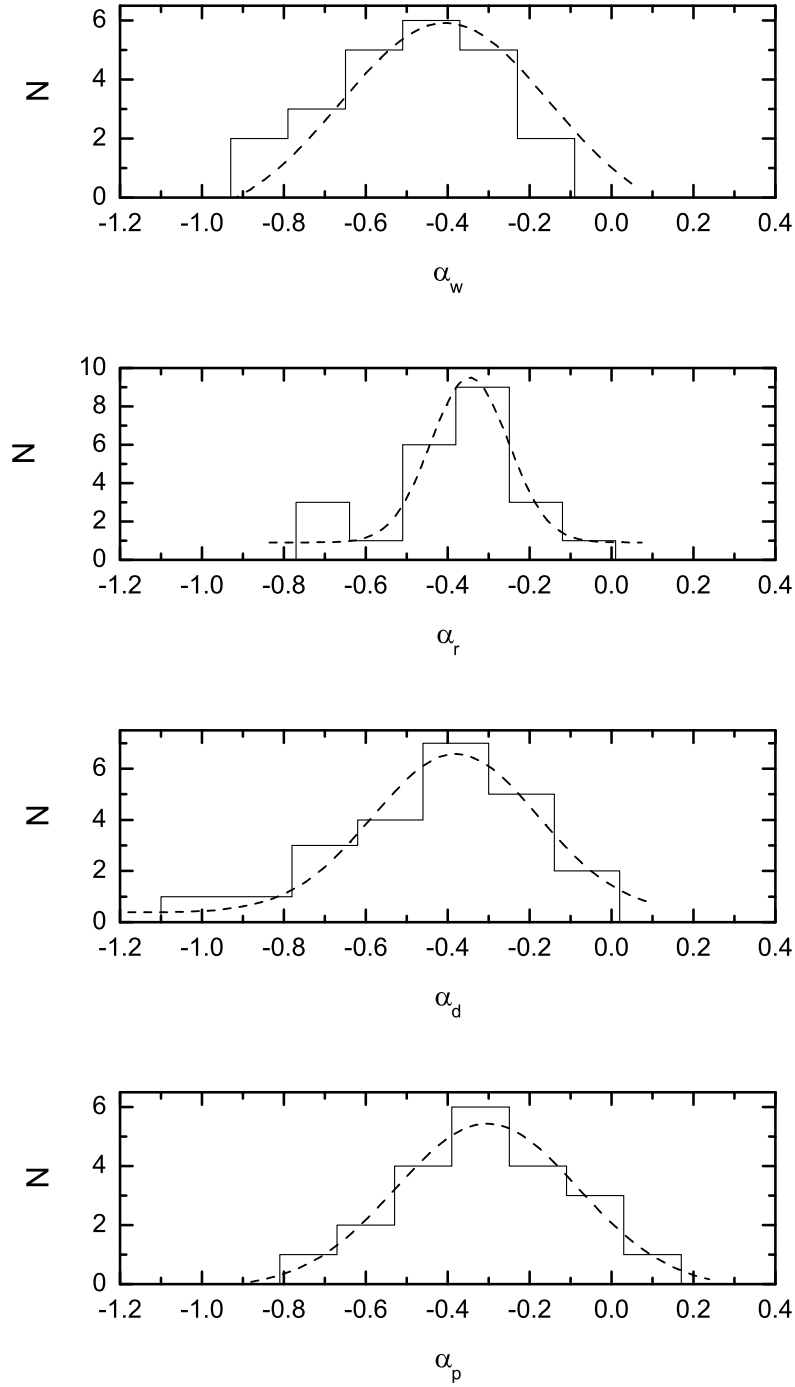


Fig. 2. Distributions of the power-law indices α_w (the first panel), α_r (the second panel), α_d (the third panel) and α_p (the fourth panel) obtained by fitting the pulse width, rise time scale, decay time scale, and peak time and energy with power law functions, respectively. The dashed lines are the best fits by the Gaussian functions.

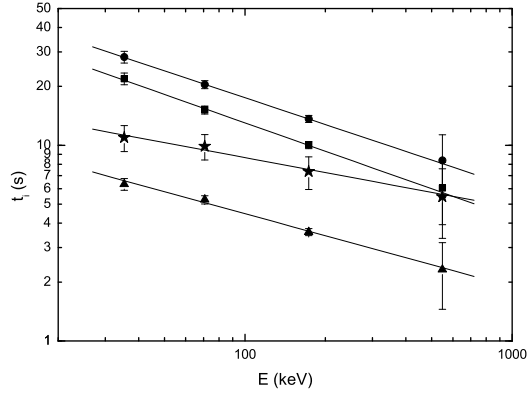


Fig. 3. The average pulse peak time (filled pentagon), width (filled circle), rise time scale (filled triangle) and decay time scale (filled square) as the functions of energy, where t_i represents the average values of t_p , Δt_w , Δt_r and Δt_d . The solid lines are the best fits.

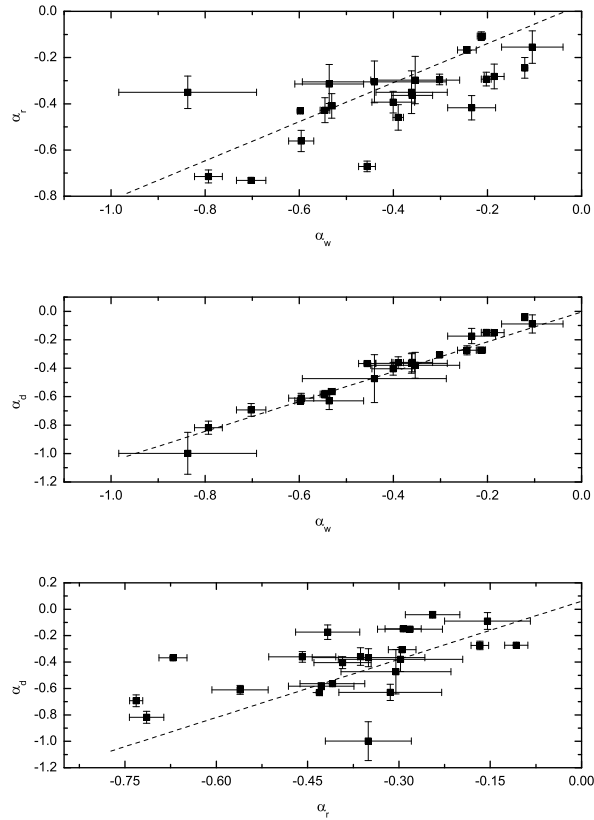


Fig. 4. Relationships between the three power-law indices α_r , α_d and α_w . The dashed lines are the regression lines.

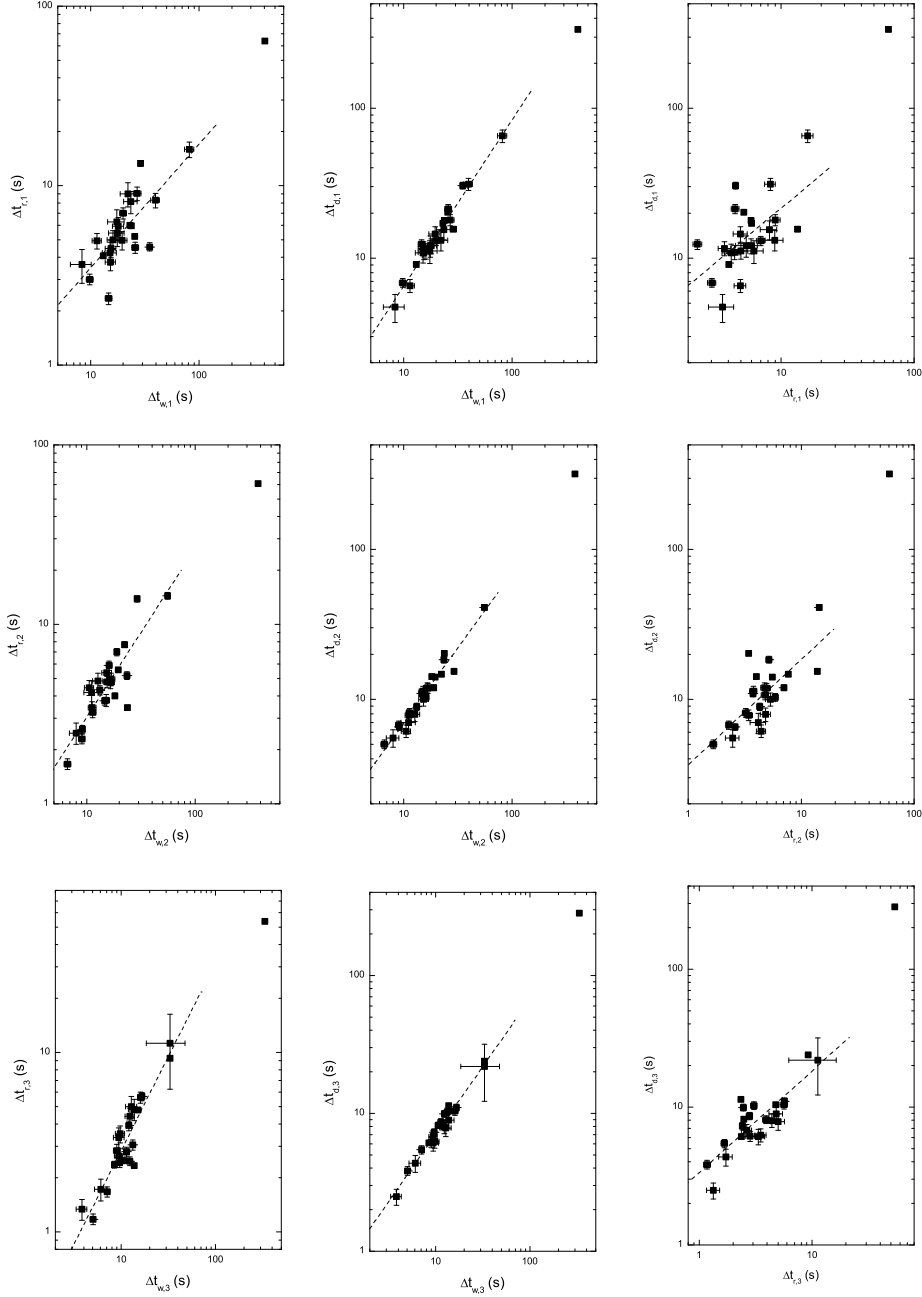


Fig. 5. Plots of Δt_r vs. Δt_w , Δt_d vs. Δt_w and Δt_d vs. Δt_r in the first three energy channels, where subscript 1, 2 and 3 represent the first channel (the first row), the second channel (the second row) and the third channel (the third row), respectively. The dashed lines are the best fits. The Δt_r are well correlated with the Δt_w in channels 1, 2, and 3 with the slopes of 0.69, 0.94 and 1.05, and $R = 0.75, 0.87, 0.92$, respectively. The Δt_d and Δt_w are strongly correlated with the slopes of 1.11, 1.01 and 0.98 and $R = 0.98, 0.98, 0.99$ for channels 1, 2, and 3, respectively. There exist the relatively weak correlations between Δt_d and Δt_r in channels 1, 2, and 3 with the slopes of 0.74, 0.70 and 0.74, and $R = 0.60, 0.74, 0.84$, respectively.

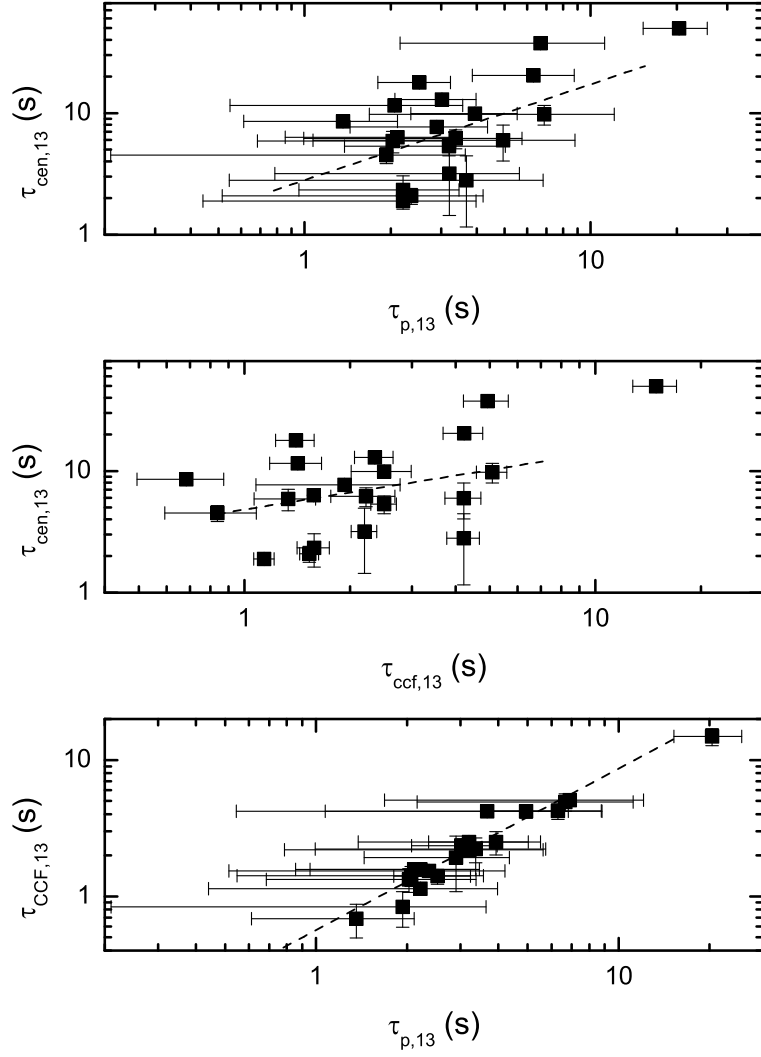


Fig. 6. Plots of the centroid lag ($\tau_{cen,13}$) vs. the peak lag ($\tau_{p,13}$), the centroid lag vs. CCF lag ($\tau_{CCF,13}$) and the CCF lag vs. the peak lag. The dashed lines are the best fits, where the correlation coefficients from the top to bottom panels are 0.44, 0.34, 0.93, respectively.

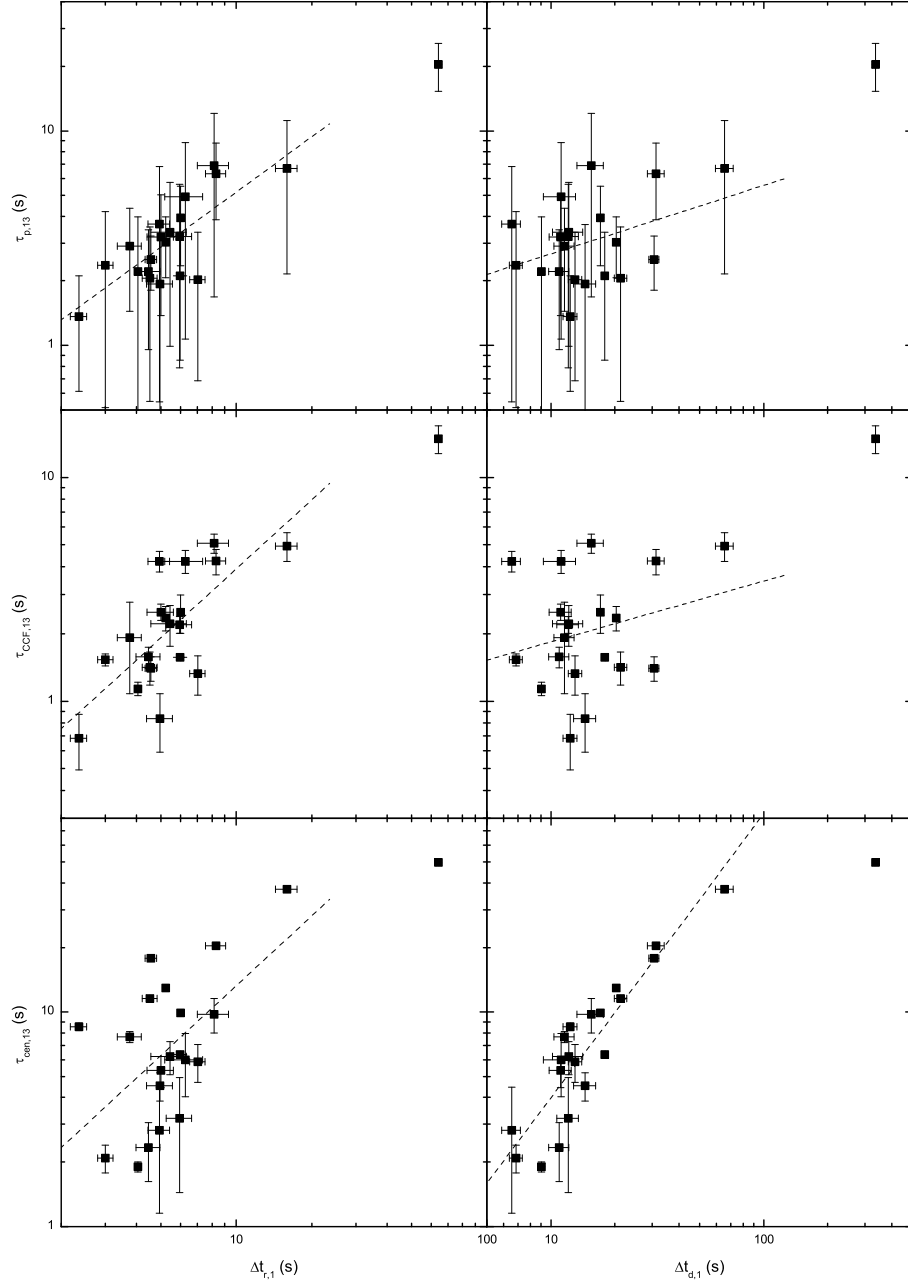


Fig. 7. Relationships between the three lags and the pulse rise time and decay time scales, where $\Delta t_{r,1}$ and $\Delta t_{d,1}$ are the pulse rise time and decay time scales in channels 1, respectively. The dashed lines are the best fits, where the correlation coefficients of between the peak lag , CCF lag and centroid lag and the pulse rise time scale are 0.76, 0.71, 0.54 (the first column), and the pulse decay time scale are 0.39, 0.25, 0.90 (the second column), respectively.

Table 1. Characteristics of the distributions of the four power-law indices.

Power-law index	Median	σ (modeled with a Gaussian)
α_p	-0.27 ± 0.04	0.45 ± 0.08
α_w	-0.39 ± 0.04	0.51 ± 0.11
α_r	-0.35 ± 0.03	0.19 ± 0.02
α_d	-0.37 ± 0.06	0.40 ± 0.06

Table 2. Correlations of the three power-law indices.

Correlation	Spearman correlation coefficient (r)	Probability (p)
$\alpha_r = (0.03 \pm 0.02) + (0.85 \pm 0.03)\alpha_w$	0.77	5.1×10^{-5}
$\alpha_d = (-0.01 \pm 0.01) + (1.05 \pm 0.03)\alpha_w$	0.98	2.2×10^{-14}
$\alpha_d = (0.06 \pm 0.03) + (1.47 \pm 0.07)\alpha_r$	0.66	1.1×10^{-3}